Above-Threshold Dissociative Ionization in the Intermediate Intensity Regime

Sujatha Unny, Yan Du, Langchi Zhu, and Robert J. Gordon
Department of Chemistry (m/c 111), University of Illinois at Chicago, 845 West Taylor Street, Chicago, Illinois 60607-7061

Akihiro Sugita and Masahiro Kawasaki
Department of Molecular Engineering, Kyoto University, Kyoto 606-8501, Japan

Yutaka Matsumi
Solar Terrestrial Environment Laboratory, Nagoya University, Toyokawa 442-8505, Japan

Tamar Seideman
Steacie Institute for Molecular Sciences, National Research Council of Canada, Ottawa K1A-0R6, Canada
(Received 12 July 2000)

The problem of dissociative ionization at intermediate intensities ($10^{10}-10^{12}$ W cm^{-2}) was studied using the example of I_2 and the technique of velocity map imaging. Several new phenomena were observed, including a continuous distribution of recoil energies peaked at zero-kinetic energy, a set of constant dissociative ionic states, and strong anisotropy of the fragment velocity distribution that is diminished by intermediate resonances.

DOI: 10.1103/PhysRevLett.86.2245 PACS numbers: 33.80.Gj, 32.80.Rm, 33.80.Eh, 33.80.Rv

Dissociative ionization (DI) is inherently interesting because it is a multibody, two-continuum process that involves both electronic and nuclear motion [1]. DI can result from collisions of molecules with either particles or photons. In the latter case, the detailed mechanism is very sensitive to the intensity and frequency of the electromagnetic field. In strong fields ($\geq 10^{14}$ W cm^{-2}), electrons are successively removed by multiple photons until the internuclear potential becomes essentially Coulombic, at which point a Coulomb explosion is ignited. Anisotropy of the angular distribution of the recoiling fragments results from the fact that the mechanism of enhanced ionization [2] depends on the angle between the symmetry axis of the neutral molecule and the polarization vector of the field. The behavior of the molecule in this limit is dominated by the properties of the field. In weak fields, a single photon is absorbed, and the superexcited molecule may decay by direct ionization, dissociation from two neutral fragments, or DI to a neutral fragment, an ion, and an electron. The anisotropy of the fragment momentum depends in this limit on the direction of the transition dipole moment of the molecule.

The present work studies the physics of DI in the previously unexplored intermediate intensity regime ($10^{10}-10^{12}$ W/cm^2), where the field and molecular Hamiltonians play equally important roles and the dynamics is inevitably richer. We find that absorption of additional photons above the threshold for dissociation leads to several new phenomena, including almost exclusively three-body fragmentation and the production of slow atoms with a highly anisotropic angular distribution.

We have used the method of velocity map imaging [3] (VMI, also known as "recoil ion momentum spectroscopy" [4]) in order to obtain both the speed and angular distribution of the fragments in a single measurement. A Nd:YAG pumped visible laser irradiated a pulsed molecular beam of target molecules seeded in 1 atm of He gas. Typical laser conditions were 30 mJ/pulse, 10 ns duration, 10 Hz repetition rate, focused with a 20 cm focal length lens to a spot size of approximately 50 μm. Product ions, produced either by DI or by postionization of fragment atoms, were focused by an electrostatic lens onto a microchannel plate (MCP) detector located 0.71 m away. The bias on the front plate of the MCP was gated to coincide with the arrival time of an ion with a selected mass/charge ratio. Electrons emitted by the MCP produced an image on a phosphor screen. The image produced by each laser shot was captured by a frame grabber connected to a CCD camera and transferred to a computer. Typically, 20 000 laser shots were averaged to produce a single two-dimensional (2D) map of the transverse recoil velocity of the gated ions. The equivalent of an inverse Abel transform generated a slice of the full three-dimensional velocity distribution of the photofragment.

We have used the VMI technique to study the DI of several iodine containing molecules in various wavelength regions. The emphasis of the present paper is on the simplest of these molecules, I_2, in the region between 556 and 575 nm. Several representative 2D images of I^+ are shown in Fig. 1. The image in Fig. 1(a) was produced at 532 nm. The single ring corresponds to the perpendicular $1u^1\Pi \leftarrow X^1\Sigma_g^+$ transition of I_2, producing two ground state $I(^2P_{3/2})$ atoms. (These atoms are ionized by absorbing six photons from the same laser pulse.) The known kinetic energy release was used to calibrate all the other images reported in this paper. Very different results were obtained at longer wavelengths. Figures 1(b)–1(d) are representative of the images recorded at nine wavelengths

 © 2001 The American Physical Society

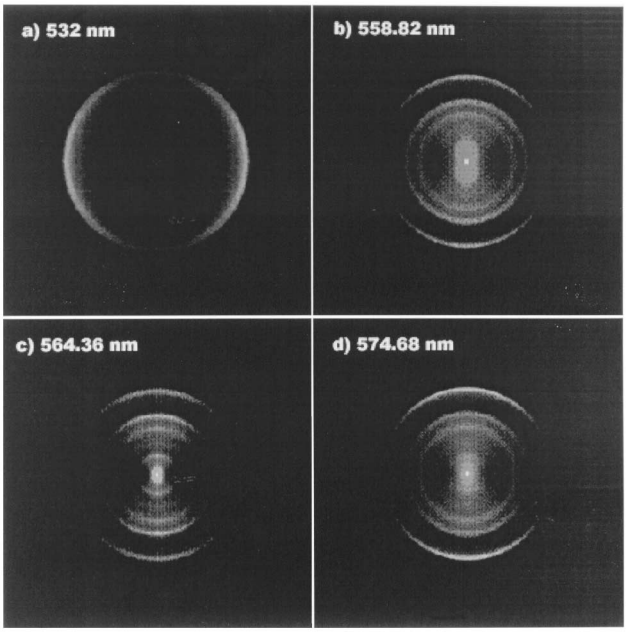

FIG. 1. 2D symmetrized images of I^+ obtained by photodissociating I_2 at (a) 532, (b) 558.82, (c) 564.36, and (d) 574.68 nm.

in the range 556–575 nm. Figures 1(b) and 1(d), taken at the two extreme wavelengths, consist of three sharp rings corresponding to parallel transitions, and an anisotropic, continuous feature peaked at zero kinetic energy. The image shown in Fig. 1(c), taken at 564.36 nm, contains at least four rings and displays much stronger channeling of the fragments along the polarization direction of the laser. Expanding the angular distributions at the peak energies in a Legendre series,

$$\mathrm{I}(\theta) = \sum_s \beta_{2s} P_{2s}(\cos\theta)\,, \qquad (1)$$

we obtain $\beta_2 \geq 2$ for the high energy ring of all the images and for all three rings at the intermediate wavelengths. In addition, we obtain nonzero values for β_4 for nearly all of the rings. These anisotropy parameters are clear evidence of multiphoton absorption [5].

Figure 2 shows the kinetic energy distributions, $p(E_t)$, for all of the images taken in this wavelength region. It is notable that, with the exception of the images taken at 564.36 and 566.00 nm, the peak positions, E_{peak}, are independent of photon energy. The vertical lines at $E_t = 0.31$, 0.49, and 0.99 eV are drawn to guide the eye and stress common peak positions, which suggest the involvement of the same transitions at different wavelengths. Also evident is a peak at zero kinetic energy at all of the wavelengths. (The scatter at the origin is caused by a singularity in the inversion procedure along the cylindrical axis of symmetry.) The wavelength dependences of E_{peak} and β_2 for the three outer rings are plotted in Fig. 3. The anisotropy of the fragments and the dip in E_{peak} at intermediate wavelengths are evident. Perhaps the most remarkable feature of Fig. 3 is the dependence of β_2 on the photon energy.

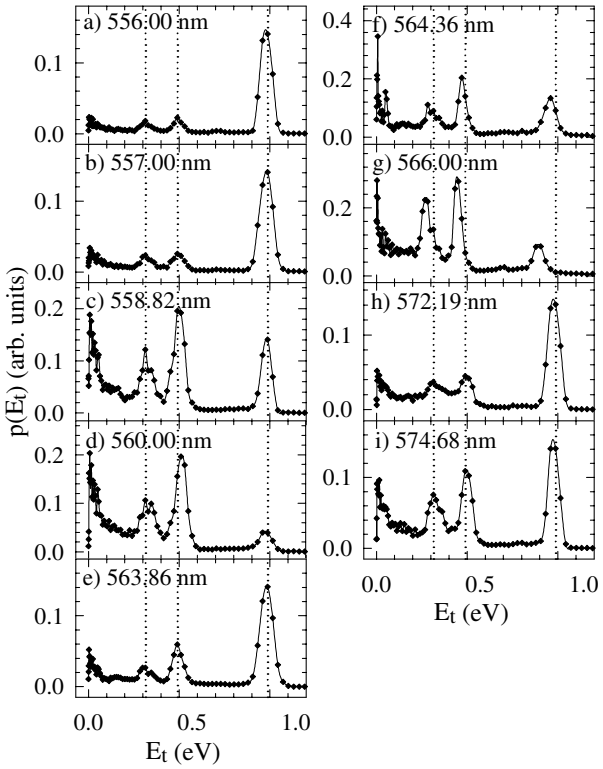

FIG. 2. Kinetic energy distributions of the I^+ fragment for different photon energies. Wavelengths are not vacuum corrected.

There is compelling evidence that the rings and central peak are caused by multiphoton DI. An attempt was made to assign the rings to direct transitions to repulsive neutral or ionic states, using the thermodynamic relation,

$$E_t = (nh\nu - D - E_1 - E_2)/2\,, \qquad (2)$$

where E_t is the laboratory kinetic energy of I^+, $2 \leq n \leq 8$ is the number of photons absorbed, D is the dissociation energy of I_2 measured with respect to the zero-point energy of the neutral molecule, and E_1 and E_2 are the asymptotic energies of the neutral and ionic fragments measured with respect to the ground neutral fragments. Included among the possible product assignments were the spin-orbit states of $\mathrm{I}(^2P_J)$ and $\mathrm{I}^+(^3P_J)$, all Rydberg series of I, and ion pairs $(\mathrm{I}^+, \mathrm{I}^-)$. Although most of the rings could be assigned to a set of products chosen from this list, the resulting mechanism attributed to each peak varies erratically with wavelength, whereas it is obvious from the similarities of the distributions in Fig. 2 that the same transitions are involved throughout. The only plausible explanation of the insensitivity of the kinetic energy distribution to the photon energy is that an electron carries off some of the available kinetic energy, which increases with photon energy. Six or more photons directly ionize I_2, with the electron carrying off sufficient energy to leave the parent ion on one of three repulsive potential energy curves [6]. [See Fig. 4(a).] To the best of our knowledge, this is the first time that a constant ionic state mechanism was observed for a repulsive

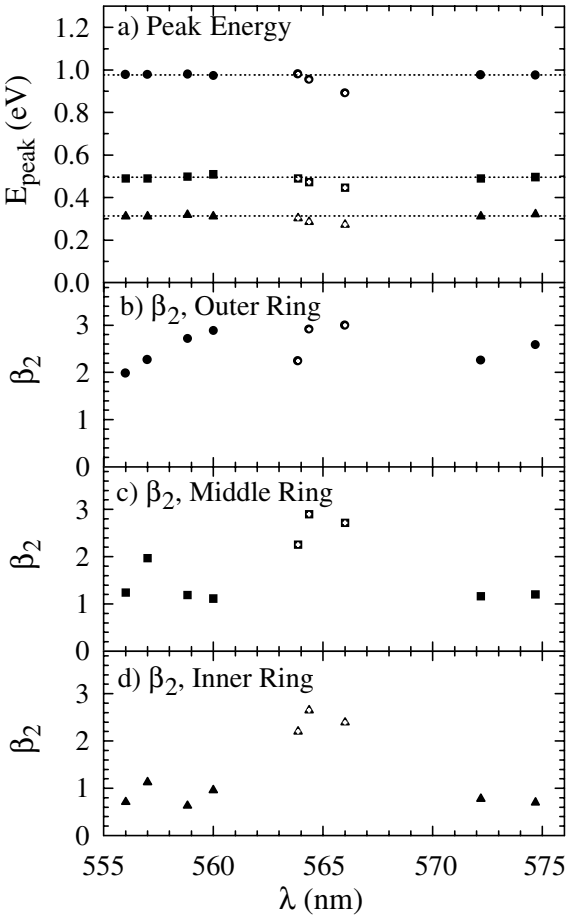

FIG. 3. Wavelength dependence of the peaks in the kinetic energy distributions [panel (a)] and the β_2 anisotropy parameter for the three outermost rings [panels (b)–(d)].

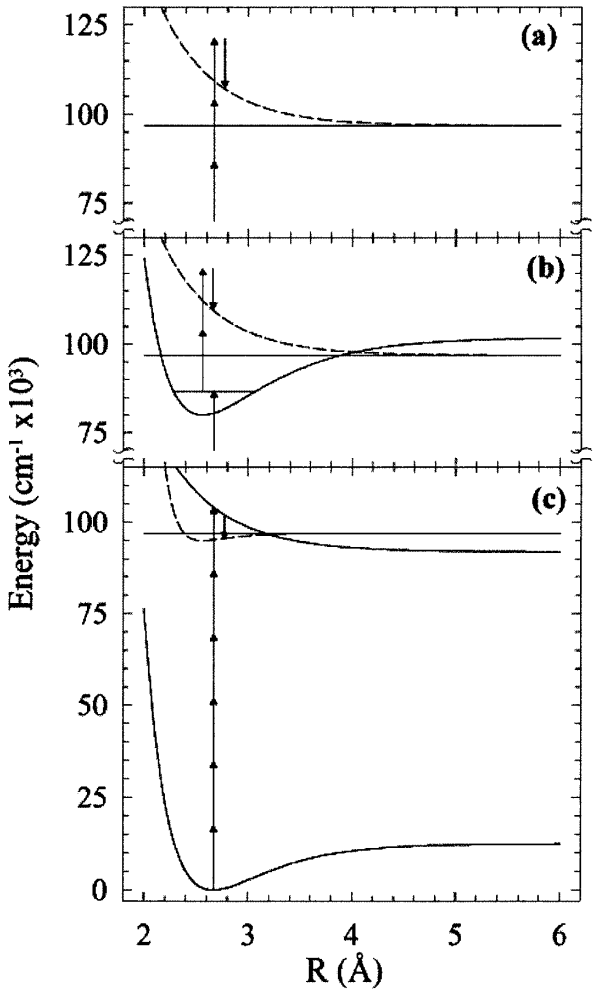

FIG. 4. Schematic drawings illustrating the mechanisms for the constant ionic states (a) without and (b) with an intermediate resonance and for (c) the zero-kinetic energy feature. To save space, the ground electronic state is depicted only in panel (c). In panels (a) and (b) seven photons directly ionize the molecule, and the electron carries off sufficient kinetic energy to leave the ion on one of three repulsive curves (only one of which is shown). If the multiphoton energy happens to match the energy of an intermediate Rydberg state [panel (b)], the remaining photons are absorbed at a smaller internuclear distance, resulting in a larger recoil energy. In the bottom panel, six photons reach a superexcited Rydberg state which autoionizes to a weakly bound ionic state. Competition between dissociation from and autoionization of the Rydberg state produces a continuous distribution of recoil energies peaked at zero. In all panels, solid curves depict neutral states and dashed curves depict ionic states. The horizontal line at 96 735 cm^{-1} indicates the DI threshold for producing ground state $I + I^+$. All but the ground state potential energy curve are schematic.

state. This behavior differs from that found for H_2 in a weak field, where the peak energies of the proton increase linearly with photon energy [7]. Further, in contrast to the weak field case [8], we observe no contribution from direct ionization of the parent molecule or from the dissociation from two neutral atoms.

In order to understand the dip in E_{peak} [see especially Fig. 2(g)] and the maxima in β_2, we measured the total ion current as a function of wavelength. The action spectrum revealed structure that is indicative of resonances present at intermediate energies. Two of these resonance structures are located between 556–561 and 571–575 nm. We tentatively attribute these features to bound Rydberg states reached with four or more photons. Because the ionic core is more tightly bound than neutral I_2, the effect of these Rydberg states is to shift the Franck-Condon window for the absorption of additional photons to shorter internuclear distances. As suggested by the schematic drawing in Fig. 4(b), the effect of the resonance is to produce a nonvertical transition to a higher point on the dissociative ionic potential energy curve, thereby converting a larger fraction of the available energy into nuclear kinetic energy. The smaller values of β_2 near resonance are expected; for rapid, direct dissociation the fragment angular distribution mirrors the anisotropy of the excitation process, whereas for slow, indirect fragmentation much of the memory of the excitation dynamics is lost by the time the fragments reach the asymptotic region, producing a much more isotropic distribution [9].

The most intriguing aspect of the images is the central, zero-kinetic energy feature. Care was taken to rule out experimental effects such as clusters, "leakage" of parent ions through the time-of-flight gate, ionization and dissociative ionization of HI molecules, the production of I_2^{2+}, and collisions within the molecular beam. The only plausible explanation of a continuous kinetic energy distribution for a diatomic molecule peaked at zero is a three-body process, with most of the available energy removed by the departing electron. The mechanism that we propose is similar to the one invoked to explain the zero-kinetic energy peak $p(E_t)$ for H_2 [10]. We postulate a six-photon excitation of a doubly excited neutral Rydberg state lying above the ionization threshold, analogous to the Q_1 and Q_2 states of H_2 [8]. Competition between dissociation from the neutral Rydberg state and autoionization to a dissociative ionic state produces a continuous distribution of ion kinetic energies [11]. If the ionic curve is flat or weakly bound in the Franck-Condon region [as sketched in Fig. 4(c)], most or all of the kinetic energy release comes from repulsion on the upper, neutral curve. Because the I atom starts out at rest (apart from its zero-point motion), $p(E_t)$ is peaked at or near zero. Photoelectron images produced from C_6H_5I [12] and NO_2 [13] are consistent with this mechanism.

The two new features observed here, the constant ionic rings and the zero-kinetic energy peak, and their insensitivity to the excitation energy, show that the molecule decays almost exclusively by a three-body process. This behavior is in stark contrast with the two-body decay mechanisms, fluorescence and neutral dissociation, observed for I_2 [14] and HI [15] in the weak field limit. A plausible mechanism is that multiphoton, above-threshold absorption allows for facile excitation of more than one electron, which is required for population of a doubly excited state. This mechanism is not limited to I_2, although the likelihood of its manifestation is enhanced by the large number of repulsive continuum states that result from the open shell structure of the halogen atom. Our observation of zero-kinetic-energy photofragments of methyl iodide and iodobenzene [12] suggests that above-threshold three-body processes are a more general phenomenon. Although the complexity of the organic parts of these molecules could lead to other modes of decay, our analysis indicates that the zero-kinetic energy peaks are due at least in part to DI.

An interesting observation is the translational energy dependence of the anisotropy of the angular distribution near the center of the image. The isotropic central spike is plausibly produced by molecules that ionize promptly and hence dissociate slowly on a weakly bound ionic potenial energy surface, as depicted in Fig. 4(c). The molecules that undergo slow autoionization recoil more rapidly on the neutral surface and therefore retain some memory of their initial alignment, producing a β_2 that increases monotonically with E_t. An intriguing alternative possibility, which we are currently investigating, is that the laser field dynamically aligns the neutral molecule [16] before it fully dissociates. The slowness of the dissociation, along with the large, positive parallel polarizability of the Rydberg state [17], which is sensitive to the internuclear distance, suggest that alignment of the neutral molecule may be possible.

In summary, we have found that the photodissociation of iodine in the intermediate intensity regime is dominated by three-body processes. We have observed several new phenomena, including direct ionization to repulsive states with constant recoil energy (independent of photon energy), the production of slow atoms with an electron carrying away most of the kinetic energy, and a highly anisotropic angular distribution that is modified by the presence of intermediate energy resonances.

We have enjoyed fruitful discussions with Dr. J. Berkowitz, Professor S. Berry, Professor R. Field, Professor A. Suits, and Dr. W. Siebrand. R. J. G. thanks the Office of Basic Energy Sciences of the Department of Energy for its generous support under Grant No. DE-FG02-98ER14880. M. K. acknowledges partial support from a "Molecular Physical Chemistry" grant funded by the Ministry of Education of Japan.

[1] R. S. Berry and S. Leach, Adv. Electron. Electron Phys. **57**, 1 (1980).
[2] T. Seideman, M. Yu. Ivanov, and P. B. Corkum, Phys. Rev. Lett. **75**, 2819 (1995).
[3] A. T. J. B. Eppink and D. H. Parker, J. Chem. Phys. **109**, 4578 (1998).
[4] R. Dorner *et al.,* Phys. Rev. Lett. **76**, 2654 (1996).
[5] R. J. Gordon and G. E. Hall, Adv. Chem. Phys. **96**, 1 (1996).
[6] The high energy peak in Fig. 2(i) (574.68 nm) lies 0.04 eV above the energy threshold for seven photons, suggesting that at least for this feature seven photons are involved.
[7] K. Ito, R. I. Hall, and M. Ukai, J. Chem. Phys. **104**, 8449 (1996).
[8] N. Kouchi, M. Ukai, and Y. Hatana, J. Phys. B **30**, 2319 (1997).
[9] M. Kawasaki, H. Sato, T. Kikuchi, A. Fukuroda, S. Kobayashi, and T. Arikawa, J. Chem. Phys. **86**, 4425 (1987).
[10] Z. X. He *et al.,* J. Chem. Phys. **103**, 3912 (1995); K. Ito *et al.,* Chem. Phys. Lett. **151**, 121 (1988); C. J. Latimer *et al.,* J. Phys. B **25**, L211 (1992); C. J. Latimer *et al.,* J. Chem. Phys. **102**, 722 (1955).
[11] A. U. Hazi, J. Chem. Phys. **60**, 4358 (1974).
[12] S. Unny *et al.,* J. Phys. Chem. A (to be published).
[13] J. A. Davies, J. E. LeClaire, R. E. Continetti, and C. C. Hayden, J. Chem. Phys. **111**, 1 (1999).
[14] L. Brewer and J. Tellinghuisen, J. Chem. Phys. **56**, 3929 (1972).
[15] M. A. Young, J. Phys. Chem. **97**, 13 508 (1993).
[16] H. Sakai, C. P. Sulfvan, J. J. Larsen, M. Hilligsøe, K. Hald, and H. Stapeldeldt, J. Chem. Phys. **110**, 10 235 (1999).
[17] T. Seideman, J. Chem. Phys. **112**, 2164 (1999).